An adaptive SIF and KF estimation strategy for fault detection based on the NIS metric

Waleed Hilal, Naseem Alsadi, Stephen Gadsden, Mohammad AlShabi

Waleed Hilal, Naseem Alsadi, Stephen A. Gadsden, Mohammad AlShabi, "An adaptive SIF and KF estimation strategy for fault detection based on the NIS metric," Proc. SPIE 12546, Sensors and Systems for Space Applications XVI, 125460S (13 June 2023); doi: 10.1117/12.2664054

SPIE.

Event: SPIE Defense + Commercial Sensing, 2023, Orlando, Florida, United States

An adaptive SIF and KF estimation strategy for fault detection based on the NIS metric

Waleed Hilal*[a], Naseem Alsadi[a], Stephen A. Gadsden[a], Mohammad AlShabi[b]
[a]McMaster University, 1280 Main St. W, Hamilton, ON, CA L8S 4L8;
[b]University of Sharjah , University City Road, Sharjah, UAE

ABSTRACT

State estimation strategies play an essential role in the effective operation of dynamic systems by extracting relevant information about the system's state when faced with limited measurement capability, sensor noise, or uncertain dynamics. The Kalman filter (KF) is one of the most commonly used filters and provides an optimal estimate for linear state estimation problems. However, the KF lacks robustness as it does not perform well in the face of modelling uncertainties and disturbances. The sliding innovation filter (SIF) is a newly proposed filter that uses a switching gain and innovation term, and unlike the KF, it only results in a sub-optimal estimate. However, the SIF has been proven to be robust to modelling uncertainties, disturbances, and ill-conditioned problems. In this work, we propose an adaptive SIF and KF (SIF-KF) estimation algorithm that can detect faulty or uncertain conditions and switch between the KF and SIF gain in the absence or presence of such conditions, respectively. A fault detection mechanism based on the normalized innovation squares (NIS) metric is also presented, which is responsible for triggering the activation of the respective gain in the proposed SIF-KF strategy. Experimental simulations are carried out on a simple harmonic oscillator subject to a fault to demonstrate the proposed SIF-KF's effectiveness over traditional approaches.

Keywords: Estimation theory, Kalman filter, sliding innovation filter, aerospace system, harmonic actuator, adaptive estimation, fault detection, signal filtering.

1. BRIEF INTRODUCTION

The Kalman filter (KF), originally introduced in the 1960s [1], has been the 'workhorse' of estimation theory and countless applications. The KF optimally solves the stochastic estimation problem for known linear systems affected by white process and measurement noise [2]. Optimality of the KF comes from the form of the gain structure and the way in which it is derived; by attempting to minimize the trace of the state error covariance. The trace is used as it represents the sum of the state errors. The impact of the KF algorithm has been widespread – leading to substantial advancements in estimation, tracking, navigation, control, and many other applications. Many well-known engineering achievements such as the Apollo space program and the global positioning system (GPS) owe their success to the KF.

Based on variable structure theory and sliding mode observers, the smooth variable structure filter (SVSF) was introduced [26]. Similar to the KF, the SVSF is formulated as a predictor-corrector estimator but utilizes a different gain structure [26], [27]. The SVSF gain is a function of the measurement errors and a switching term [26]. The switching structure of the gain brings an inherent amount of stability to the estimation process as its bounds the estimates to the trajectory of the true state values [2], [28]. However, the SVSF as presented in [26] did not contain a state error covariance derivation. The SVSF was expanded in [2], [27], [29] to contain a covariance function which increased the number of useful applications for the filter. Other improvements were also presented that included the use of a chattering function for fault detection, higher-order solutions, and multi-target tracking formulations [12], [30]–[33].

Given the optimal VBLs reduction of the SVSF to a KF, a hybrid approach was proposed. Termed the SVSF-VBL or alternately the SVSF-KF, the resultant is an estimation strategy that would provide the more optimal KF estimate during normal system operation and that of the SVSF in the presence of a fault. The VBL was used as a detection/switching mechanism, where a sudden increase in the VBL width beyond a designer specified threshold would control activation of the SVSF gain. The SVSF-KF was successfully demonstrated in multiple cases [3]–[11], and several non-linear extensions were advanced based on the extended Kalman filter (EKF), the unscented Kalman filter (UKF), and the cubature Kalman filter (UKF). These were termed the SVSF-EKF, SVSF-UKF, and SVSF-CKF respectively.

Sensors and Systems for Space Applications XVI, edited by Genshe Chen,
Khanh D. Pham, Proc. of SPIE Vol. 12546, 125460S · © 2023 SPIE
0277-786X · doi: 10.1117/12.2664054

In this paper, the sliding innovation filter (SIF) is investigated. The SIF is based on variable structure techniques similar to the SVSF and sliding mode observers, however its gain structure is simpler and it provides more accurate results while maintaining robustness. Note also that the SIF may be combined with control strategies for improved tracking performance and robustness to uncertainties and disturbances. Specifically, this paper investigates replacing the SVSF in the adaptive SVSF-KF strategy with the SIF.

The remainder of this paper is organized as follows: a background on the Kalman filter, sliding innovation filter and estimation problem is detailed in Section 2. Then, the methodology behind the proposed research is outlined in Section 3, followed by a detailed discussion of the results in Section 4, Finally, concluding remarks and suggestions for future work are provided in Section 5.

2. BACKGROUND

2.1 Kalman filter

Linear dynamic systems can be expressed in state-space representation as follows [12], [13]:

$$\boldsymbol{x}_{k+1} = \boldsymbol{A}\boldsymbol{x}_k + \boldsymbol{B}\boldsymbol{u}_k + \boldsymbol{w}_k \tag{1}$$

$$\boldsymbol{z}_k = \boldsymbol{H}\boldsymbol{x}_k + \boldsymbol{v}_k \tag{2}$$

where $\boldsymbol{x}$ represents the system state vector, $\boldsymbol{A}$ is the discretized linear system model matrix of differential equations, $\boldsymbol{B}$ is the input gain matrix, $\boldsymbol{u}$ is the input vector, $\boldsymbol{w}$ is the system noise, $\boldsymbol{z}$ is the measurement vector, $\boldsymbol{H}$ is the linear measurement matrix, $\boldsymbol{v}$ represents the measurement noise, and k represents the current timestep.

The Kalman filter (KF) works under the assumptions that the system model is relatively well-known, and the initial states are also known, and finally, that the system and measurement noise is normal and Gaussian meaning that it is white with zero mean and known respective covariance matrices [2]. The KF works as a predictor-corrector; the system model is used to obtain an *a priori* or predicted estimate of the states, whereupon measurements combined with the Kalman gain matrix are used to apply a correction term to create an *a posteriori* or updated state estimate [14], [15].

The *a priori* state estimate is first computed using the process model, as can be seen in (3). Then, the *a priori* state covariance matrix is calculated based on the process model and the associated modeling noise covariance matrix $\boldsymbol{Q}_k$, as shown in (4):

$$\widehat{\boldsymbol{x}}_{k+1|k} = \boldsymbol{A}\widehat{\boldsymbol{x}}_{k+1|k} + \boldsymbol{B}u_k \tag{3}$$

$$\widehat{\boldsymbol{P}}_{k+1|k} = \boldsymbol{A}\boldsymbol{P}_{k|k}\boldsymbol{A}^T + \boldsymbol{Q}_k \tag{4}$$

The Kalman gain computation in (5) is based on (4), and is then used to update the state estimate in (6):

$$\boldsymbol{K}_{k+1} = \boldsymbol{P}_{k+1|k}\boldsymbol{H}^T\boldsymbol{S}_{k+1}^{-1} \tag{5}$$

$$\widehat{\boldsymbol{x}}_{k+1|k+1} = \widehat{\boldsymbol{x}}_{k+1|k} + \boldsymbol{K}_{k+1}\boldsymbol{\nu}_{k+1} \tag{6}$$

where $\boldsymbol{\nu}$ and $\boldsymbol{S}$ are two important terms known as the innovation (or residual), and the innovation covariance, respectively. In the equations below, $\boldsymbol{R}$ is the measurement noise covariance.

$$\boldsymbol{\nu}_{k+1} = \boldsymbol{z}_k - \boldsymbol{H}\boldsymbol{A}\hat{\boldsymbol{x}}_{k+1|k} \tag{7}$$

$$\boldsymbol{S}_{k+1} = \boldsymbol{H}\boldsymbol{P}_{k+1|k}\boldsymbol{H}^T + \boldsymbol{R}_{k+1} \tag{8}$$

The innovation, from (7), represents the difference between the actual measurements and the *a priori* estimate of the measurements. The innovation covariance, as in (8), characterizes the uncertainty in the measurement predictions. These two terms provide an important insight into the estimation process and are often used to assess the filter's overall estimation ability.

The *a posteriori* state error covariance matrix is then calculated in (9), and the process repeats iteratively:

$$\boldsymbol{P}_{k+1|k+1} = (\boldsymbol{I} - \boldsymbol{K}_{k+1}\boldsymbol{H})\boldsymbol{P}_{k+1|k}(\boldsymbol{I} - \boldsymbol{K}_{k+1}\boldsymbol{H})^T + \boldsymbol{K}_{\boldsymbol{k+1}}\boldsymbol{R}_{\boldsymbol{k+1}}\boldsymbol{K}_{\boldsymbol{k+1}}^T \tag{9}$$

where $\boldsymbol{I}$ is the identity matrix. In a successful application of the KF, the state estimates will rapidly converge, providing the optimal statistical estimate based on the given information. The *a posteriori* covariance update in (9) is known as the 'Joseph covariance form' and is often preferred due to its superior numerical characteristics. The Joseph form ensures that the covariance update remains positive-definite, a critical condition in the estimation process to produce meaningful results [2].

2.2 Sliding innovation filter

Similar to the KF, the sliding innovation filter (SIF) is formulated as a predictor-corrector estimation method [16]–[21]. First, the prediction stage involves computing the *a priori* state estimates and state error covariance, and then the predicted innovation as follows:

$$\hat{\boldsymbol{x}}_{k+1|k} = \boldsymbol{A}\hat{\boldsymbol{x}}_{k|k} + \boldsymbol{B}u_k \tag{10}$$

$$\hat{\boldsymbol{P}}_{k+1|k} = \boldsymbol{A}\boldsymbol{P}_{k|k}\boldsymbol{A}^T + \boldsymbol{Q}_k \tag{11}$$

$$\tilde{\boldsymbol{z}}_{k+1|k} = \boldsymbol{z}_{k+1} - \boldsymbol{H}\hat{\boldsymbol{x}}_{k+1|k} \tag{12}$$

In the update stage, the SIF gain $\boldsymbol{K}_{k+1}$ is computed and used in the computation of the *a posteriori* state estimates and state error covariance as follows:

$$\boldsymbol{K}_{k+1} = \boldsymbol{H}^{+}\overline{sat}(\left|\tilde{\boldsymbol{z}}_{k+1|k}\right|/\,\delta) \tag{13}$$

$$\hat{\boldsymbol{x}}_{k+1|k+1} = \hat{\boldsymbol{x}}_{k+1|k} + \boldsymbol{K}_{k+1}\tilde{\boldsymbol{z}}_{k+1|k} \tag{14}$$

$$\boldsymbol{P}_{k+1|k+1} = (\boldsymbol{I} - \boldsymbol{K}_{k+1}\boldsymbol{H})\boldsymbol{P}_{k+1|k}(\boldsymbol{I} - \boldsymbol{K}_{k+1}\boldsymbol{H})^T + \boldsymbol{K}_{\boldsymbol{k+1}}\boldsymbol{R}_{\boldsymbol{k+1}}\boldsymbol{K}_{\boldsymbol{k+1}}^T \tag{15}$$

Note that $\boldsymbol{H}^{+}$ refers to the pseudoinverse of the measurement matrix, $\overline{sat}$ refers to the diagonal of the saturation term, sat refers to the saturation term of a value (yielding results between -1 and +1), $\left|\tilde{\boldsymbol{z}}_{k+1|k}\right|$ refers to the absolute value of the innovation, δ refers to the sliding boundary layer width, and $\boldsymbol{I}$ refers to the identity matrix.

The main difference between the KF and the SIF is in the structure of the gain. For the KF, the gain is derived as a function of the state error covariance, which offers optimality. However, for the SIF, the gain is instead based on the

measurement matrix, the innovation, and a sliding boundary layer term. While the state error covariance is not involved in the computation of the SIF gain, it still provides useful information as it represents the amount of estimation error in the filtering process. An overview of the SIF estimation concept is illustrated in Fig. 1. From this figure, it can be seen that an initial estimate is pushed towards the sliding boundary layer, which is defined based on the degree of uncertainty present in the estimation process. Once within the sliding boundary layer, the estimates are forced to switch about the true state trajectory of the SIF gain.

2.3 Adaptive formulation of KF and SIF

During normal operation, the boundary layer generally converges to a size proportional to the amount of assumed process noise. In the presence of a system change the boundary layer will rapidly expand. With this in mind, a hybrid strategy was proposed to combine the SIF and KF using the boundary layer as a mechanism to detect system change [22]. However, issues have been observed in that the boundary layer results in a high frequency switching between the two filters due to the presence of chattering. In response to this issue, we proposed and consider an alternative fault detection strategy based on the normalized innovation squares (NIS) metric [13].

The NIS is simply the square innovation vector at a given time-step, normalized by the innovation covariance. It can be expressed as follows:

$$\boldsymbol{r_k} = \boldsymbol{\nu}_k^T \boldsymbol{S}_k^{-1} \boldsymbol{\nu_k} \tag{16}$$

Under the assumption of white Gaussian noise, with an accurately modeled system, a Kalman filter's innovations are characterized by several important statistical properties. These properties of the innovations are that they are white, zero means and have a known covariance. When the filter's model no longer accurately represents the system's dynamics in reality, the innovations will violate these conditions. Consequently, the innovations will, in many cases, begin to grow, and thus can be used a means of detecting filter divergence [12], [23]–[25].

In this paper, we shall consider the basic threshold approach outlined in [12] for target maneuver detection. In tracking filters, a target maneuver represents a sudden change to the system model, which if unaccounted for can lead to filter divergence. Methods used for target maneuver detection are readily applicable to other estimation applications where system change is a concern.

An NIS-based SIF-KF involves monitoring the innovations, such that if they grow beyond a designer defined limit, a system change is assumed, and the SIF gain is triggered [25]. A reasonable threshold can be defined based on the knowledge that the NIS in an optimal, matched filter, and characterized by a chi-squared distributed with the number of degrees of freedom equal to the number of measurements *N*.

$$\boldsymbol{r} \sim \chi_N^2 \tag{17}$$

The robustness can further be improved by averaging a sequence of the innovation history. This will help smooth out any 'noise' in the innovations and avoid false detections. In addition, to avoid an erratic switching effect across a single threshold line, two thresholds with a hysteresis approach can be arranged: a higher "on" threshold such that false triggers of the SIF are avoided, and a lower "off" threshold, to be triggered once the innovations drop back to normal.

Two basic sequence averaging techniques may be considered: the sliding window average, and the fading memory average. In the sliding window average, the most recent *w* innovations are averaged, with all prior innovations being ignored. In a fading memory average, the entire innovation history is included, with the more distant innovations weighted exponentially lower. The weights are determined by a forgetting factor α where $0 < \alpha < 1$.

The sliding window and fading memory average approaches can be expressed mathematically in equations (18) and (19) respectively [3], [12]:

$$\boldsymbol{r_k^w} = \sum_{\boldsymbol{j=k-w+1}}^{\boldsymbol{k}} \boldsymbol{r_k} \tag{18}$$

$$\boldsymbol{r_k^\alpha} = \alpha \boldsymbol{r_{k-1}^\alpha} + \boldsymbol{r_k} \tag{19}$$

In our studies, we make use of the fading memory average. In an optimally modeled filter, the fading memory average of the NIS will also have an approximately chi-squared distribution with number of degrees of freedom related to N and α as follows [12]:

$$dof\chi = \frac{N}{1-\alpha} \tag{20}$$

The thresholds can then be defined based on an appropriate chi-squared tail probability. For example, a system with three states and a memory factor of α = 0.965, will result in an expected chi-squared distribution with 92 degrees-of-freedom. A tail probability of 0.001, reflecting an unexpected innovation sequence, would translate into an "on" threshold of about 140.

3. METHODOLOGY

The performances of our newly proposed SIF-KF approach, which we call the NIS SIF-KF, is tested in experimental simulations involving the simple linear situation described as follows. We shall consider an underdamped simple harmonic oscillator subject to a fault condition. The system's state space equations can be expressed as:

$$\begin{bmatrix} \dot{x} \\ \dot{v} \end{bmatrix} = \begin{bmatrix} 0 & 1 \\ -\frac{k}{m} & -\frac{c}{m} \end{bmatrix} \begin{bmatrix} x \\ v \end{bmatrix} \tag{21}$$

where k is the spring constant, m is the mass, c is the damping coefficient, and x and v are the position and velocity states, respectively.

We simulate this system with an initial mass of $15\ kg$, $5\ N/m$ spring constant, and $0.5\ Ns/m$ damping coefficient. After 30 seconds, a sudden system change occurs and the mass increases to $35\ kg$ and the damping coefficient to $2\ Ns/m$. Artificial measurement noise is simulated that is of Gaussian distribution with zero mean and a variance of 0.001, and otherwise, we assume no significant process noise. We consider two basic test scenarios, one with a permanent fault, and one with just a temporary fault.

In our simulations, we simulate the free response of a simple mass-spring-damper system. As in the previous simulation, after 30 seconds the mass suddenly increases from $15\ kg$ to $35\ kg$, and the damping coefficient from $0.5\ Ns/m$ to $2\ Ns/m$. Full measurements are available, and the measurement noise variance is 0.001 for both states. Otherwise, no significant process noise is considered. The sampling rate used for the simulation is $T = 1$ ms.

For the SIF-based estimates, a smoothing boundary layer width vector is set based on trial-and-error tuning as:

$$\boldsymbol{\Psi} = \begin{bmatrix} 1 \\ 0.2 \end{bmatrix} \tag{22}$$

For the VBL-based SIF-KF, an SBL limit of 50 is used, based on the position state. For the NIS SIF-KF, triggering thresholds of 140 for "on" and 120 for "off" were used. These values represent tail probabilities of 0.001 and 0.05, respectively, which correspond to a memory factor of α = 0.965 and 92 degrees of freedom.

4. RESULTS AND DISCUSSION

First under consideration is the performance of the filters upon the introduction of a permanent fault halfway through the simulation. The overall performance of each filter is compared by simulating 500 Monte Carlo runs of the scenario in study. The average RMSE of each filter for the position state estimate is recorded for three intervals of the simulations: prior to the fault $t < 30s$, after the fault $t \geq 30s$, and throughout the entire simulation $0 \leq t \leq 60s$. The results of the first test case, where a permanent fault is introduced, are presented in Table I.

When examining the performances of the filters prior to the fault, it can be seen that the KF, SIF-KF and NIS SIF-KF are all equally the best performing filters. This result is as one would expect, since the KF provides an optimal estimate, and since NIS SIF-KF is able to maintain its gain activation at the KF. However, the KF is the worst performing filter during the fault, and overall. Upon the introduction of the fault, the SIF-KF's performance degrades significantly, resulting in it being the second worst filter overall. As for the SIF, it demonstrates its characteristic robustness during the fault, with a suboptimal pre-fault estimate.

Regardless, NIS SIF-KF demonstrates the best overall performance of all the studied filters, followed by the SIF. The NIS SIF-KF performs the best during the faulty conditions but provides a suboptimal estimate prior to the fault. Compared to the original boundary layer-based SIF-KF, the NIS SIF-KF represents an improvement of 85.8 percent.

The gain activation of the NIS SIF-KF is plotted in Fig. 1 for further examination of its switching performance. It can be seen in the figure that the NIS-based detection scheme can recognize and account for the fault shortly after its occurrence by switching to and maintaining the SIF gain for the remainder of the simulation. In fact, the NIS-based approach detects the fault within approximately 2.3 seconds of its occurrence. Furthermore, it can be observed that the NIS approach can maintain the SIF gain and eliminate the high-frequency switching behaviour associated with the original SIF-KF method. In Fig. 1, the red line indicates the "on" threshold for the SIF gain activation, and the green line indicates the "off" threshold.

TABLE I
RMSE OF STUDIED MODELS IN THE CASE OF A PERMANENT FAULT

Model	KF	SIF	SIF-KF	NIS SIF-KF
$t < 30s$	0.0033	0.0073	0.0033	0.0033
$t \geq 30s$	0.521	0.0313	0.1822	0.0254
$0 \leq t \leq 60s$	0.413	0.0298	0.1621	0.0229

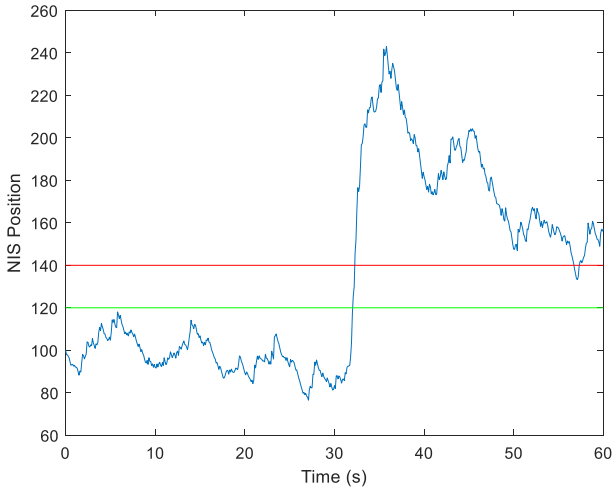

Figure 1. NIS of the position state in the permanent fault scenario. Red and green lines indicate the "on" and "off" thresholds, respectively, for the SIF gain.

The next simulation considers a similar scenario to the one previously examined and discussed, except that the modeling change is temporary and resolved 30 seconds after its introduction. As in the previous trials, 500 Monte Carlo runs of the scenario in study were carried out and the RMSE results of the position estimates for all filters are recorded, as can be seen in Table II. Note that this table also considers the RMSE value after the fault, where $60 \leq t \leq 100s$. From Table II, it is clear that the KF performs the worst overall for the entire course of the simulation, followed by the SIF-KF. Despite this, the KF demonstrates the lowest RMSE prior to the fault or modeling change, tied with both the SIF-KF and the NIS SIF-KF. The best overall performer is the NIS SIF-KF.

It can thus be inferred that despite the NIS SIF-KF's slower response to detecting the start and end of the modeling change, it is still able to perform robustly enough to outperform all the other filters. Overall, the NIS SIF-KF represents an improvement of 88.6 percent compared to the boundary layer-based SIF-KF.

In Figure 2, the NIS values of the position state are shown, along with the mechanism behind the detection of system change. From this figure, the effectiveness of the gain activation scheme is further validated, especially in the rapidness of its detection of the fault. However, it can be inferred the NIS is somewhat slow in determining the fault's cessation. Approximately 10 seconds elapse before the NIS value crosses below the "off" threshold to switch to the KF gain. Thus, it may prove worthwhile for future research effort and attention to be directed towards the adjustment of the NIS thresholds to further improve the performance of the approach in this regard. Albeit, careful consideration is required for this, as the risk of increased false positives or negatives is not negligible.

TABLE II
RMSE OF STUDIED MODELS IN THE CASE OF A TEMPORARY FAULT

Model	KF	SIF	SIF-KF	NIS SIF-KF
$t < 30s$	0.0029	0.0104	0.0029	0.0029
$30 \leq t \leq 60s$	0.4406	0.0214	0.1570	0.0214
$60 \leq t \leq 100s$	0.0646	0.0103	0.0617	0.0070
$0 \leq t \leq 100s$	0.2937	0.0171	0.1335	0.0152

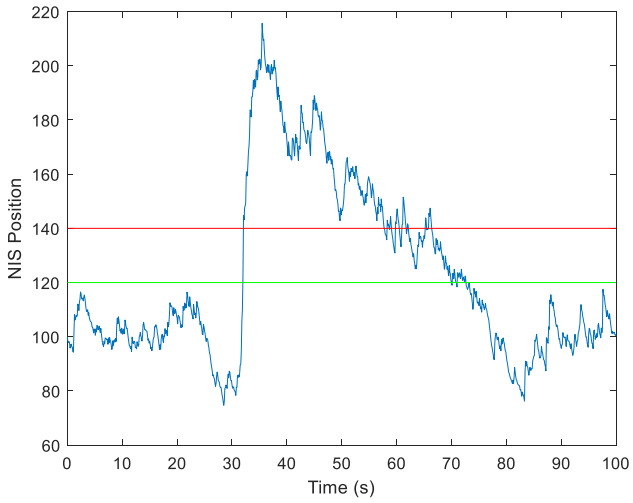

Figure 2. NIS of the position state in the temporary fault scenario. Red and green lines indicate the "on" and "off" thresholds, respectively, for the SIF gain.

5. CONCLUSION

Adaptive estimation strategies such as the SIF-KF work by providing an optimal KF estimate in normal operating conditions, and a suboptimal but robust SIF estimate in the presence of faulty operating conditions. The SIF-KF uses a boundary layer-based gain mechanism to detect the presence of faulty conditions and switch between the KF and SIF. However, the boundary layer-based gain has been shown in the literature to be easily succumbed to chattering. As a result, high frequency switching between the two filters is often observed, resulting in a significant degradation of the SIF-KF's performance. Addressing this issue, this paper proposed a new approach known as the NIS SIF-KF. We conduct an experimental simulation to compare and quantify the improved estimation performance of this approach compared to the SIF-KF when a system is afflicted with a fault.

The results of our simulations prove that the newly proposed NIS and SIF-KF outperform the existing SIF-KF approach. Specifically, the NIS SIF-KF excelled in determining when to select the optimal KF estimate or the robust SIF estimate. Further improvements to the NIS SIF-KF may also be realized by future research directed towards a more careful approach to the tuning of the fading memory parameter and switching thresholds for more rapid detection of faults.

6. REFERENCES

[1] R. E. Kalman, "A New Approach to Linear Filtering and Prediction Problems," *Journal of Basic Engineering*, vol. 82, no. 1, pp. 35–45, Mar. 1960, doi: 10.1115/1.3662552.

[2] M. S. Grewal and A. P. Andrews, *Kalman Filtering: Theory and Practice with MATLAB®: Fourth Edition*, vol. 9781118851210. 2014. doi: 10.1002/9781118984987.

[3] S. Gadsden, "Smooth Variable Structure Filtering: Theory and Applications," McMaster University, Hamilton, Ontario, 2011.

[4] S. A. Gadsden, S. Habibi, and T. Kirubarajan, "Kalman and smooth variable structure filters for robust estimation," *IEEE Trans Aerosp Electron Syst*, vol. 50, no. 2, 2014, doi: 10.1109/TAES.2014.110768.

[5] S. A. Gadsden and T. Kirubarajan, "Development of a variable structure-based fault detection and diagnosis strategy applied to an electromechanical system," in *Signal Processing, Sensor/Information Fusion, and Target Recognition XXVI*, 2017. doi: 10.1117/12.2262570.

[6] F. Demim, S. Benmansour, N. Abdelkrim, A. Rouigueb, M. Hamerlain, and A. Bazoula, "Simultaneous localisation and mapping for autonomous underwater vehicle using a combined smooth variable structure filter and extended kalman filter," *Journal of Experimental and Theoretical Artificial Intelligence*, 2021, doi: 10.1080/0952813X.2021.1908430.

[7] M. Al-Shabi and K. S. Hatamleh, "The unscented smooth variable structure filter application into a robotic arm," in *ASME International Mechanical Engineering Congress and Exposition, Proceedings (IMECE)*, 2014. doi: 10.1115/IMECE2014-40118.

[8] H. Zhou, Y. Xia, and Y. Deng, "A new particle filter based on smooth variable structure filter," *Int J Adapt Control Signal Process*, vol. 34, no. 1, 2020, doi: 10.1002/acs.3067.

[9] W. Chen, H. Zhou, F. Shen, and Z. Guo, "Current statistic model and adaptive tracking algorithm based on Kalman and Smooth Variable Structure Filters," in *9th International Conference on Microwave and Millimeter Wave Technology, ICMMT 2016 - Proceedings*, 2016. doi: 10.1109/ICMMT.2016.7762534.

[10] W. Youn and S. Andrew Gadsden, "Combined quaternion-based error state kalman filtering and smooth variable structure filtering for robust attitude estimation," *IEEE Access*, vol. 7, 2019, doi: 10.1109/ACCESS.2019.2946609.
[11] B. M. Dyer, T. R. Smith, S. A. Gadsden, and M. Biglarbegian, "Filtering Strategies for State Estimation of Omniwheel Robots," in *2020 IEEE International Conference on Mechatronics and Automation, ICMA 2020*, 2020. doi: 10.1109/ICMA49215.2020.9233826.
[12] Y. Bar-Shalom, X.-R. Li, and T. Kirubarajan, *Estimation with Applications to Tracking and Navigation*. 2001. doi: 10.1002/0471221279.
[13] J. Goodman, W. Hilal, S. A. Gadsden, and C. D. Eggleton, "Adaptive SVSF-KF estimation strategies based on the normalized innovation square metric and IMM strategy," *Results in Engineering*, vol. 16, 2022, doi: 10.1016/j.rineng.2022.100785.
[14] W. Hilal, S. A. Gadsden, S. A. Wilkerson, and M. A. Al-Shabi, "A square-root formulation of the sliding innovation filter for target tracking," 2022. doi: 10.1117/12.2618965.
[15] W. Hilal, S. A. Gadsden, S. A. Wilkerson, and M. A. Al-Shabi, "Combined particle and smooth innovation filtering for nonlinear estimation," 2022. doi: 10.1117/12.2618973.
[16] S. Andrew Gadsden and M. Al-Shabi, "The Sliding Innovation Filter," *IEEE Access*, vol. 8, 2020, doi: 10.1109/ACCESS.2020.2995345.
[17] M. Al-Shabi, S. A. Gadsden, M. El Haj Assad, and B. Khuwaileh, "A multiple model-based sliding innovation filter," 2021. doi: 10.1117/12.2587343.
[18] A. S. Lee, S. A. Gadsden, and M. Al-Shabi, "An Adaptive Formulation of the Sliding Innovation Filter," *IEEE Signal Process Lett*, vol. 28, 2021, doi: 10.1109/LSP.2021.3089918.
[19] N. Alsadi *et al.*, "Neural network training loss optimization utilizing the sliding innovation filter," 2022. doi: 10.1117/12.2619029.
[20] M. Al-Shabi, S. A. Gadsden, M. El Haj Assad, B. Khuwaileh, and S. Wilkerson, "Application of the sliding innovation filter to unmanned aerial systems," 2021. doi: 10.1117/12.2587346.
[21] S. A. Gadsden, M. Al-Shabi, and S. A. Wilkerson, "Development of a second-order sliding innovation filter for an aerospace system," 2021. doi: 10.1117/12.2587334.
[22] J. Goodman, S. A. Wilkerson, C. Eggleton, and S. A. Gadsden, "A multiple model adaptive SVSF-KF estimation strategy," 2019. doi: 10.1117/12.2520018.
[23] A. Gelb, *Applied optimal estimation*, vol. 64, no. 4. 2001.
[24] P. S. Maybeck, "Stochastic models, estimation, and control - Introduction," in *Stochastic models, estimation, and control*, 1979.
[25] Y. Qin, Y. Liang, Y. Yang, F. Yang, and X. Wang, "A nonlinear filter switch method based on normalized innovation square," in *Chinese Control Conference, CCC*, 2013.